

PSFC/JA-02-22

**Resistive MHD Transport Model for
an RFP
Part I – The Model**

A. Bruno, J.P. Freidberg,* R.J. Hastie

October 2002

Plasma Science and Fusion Center
Massachusetts Institute of
Technology
Cambridge, MA 02139 USA

*Massachusetts Institute of
Technology
Department of Nuclear Engineering
Room 24-107
Cambridge, MA 02139

This work was supported by the U.S. Department of Energy, Grant No. DE-FG02-91ER-54109. Reproduction, translation, publication, use and disposal, in whole or in part, by or for the United States government is permitted.

Submitted for publication to *Physics of Plasmas*

I Introduction

The Reversed Field Pinch (RFP) concept offers several attractive features with respect to an ultimate fusion power reactor as compared to a tokamak [1]. The RFP is potentially capable of high β operation with a large fraction of the ignition heating provided by ohmic current. The net result is a compact, high power density reactor which should lead to a lower capital cost. However, achieving this high performance has been difficult experimentally. In particular the energy confinement time is typically much shorter in an RFP than in a tokamak. As a consequence a major focus of current RFP research is aimed at understanding and improving energy confinement.

The present work is aimed at developing a self consistent theory of energy confinement in an ohmically heated RFP. The primary goal is to determine the magnitude and radial dependence of the anomalous perpendicular thermal diffusivity $\chi_{\perp}(r)$ as well as the corresponding macroscopic scaling relations for τ_E and β_p . The basic idea is to extend Taylor's theory of relaxation [2] to include the effects of an external heat source (i.e. ohmic heating). Recall that in Taylor's theory, resistive MHD turbulence causes the plasma to relax to a minimum energy state in which the plasma pressure gradient vanishes and the resulting force free configuration satisfies $\mathbf{j} = \mu\mathbf{B}$ with $\mu = \text{const}$. The present model allows the inclusion of a heat source, which drives the plasma pressure gradient away from zero. The pressure then rises until the input power is balanced by the outward heat conduction losses. If the thermal diffusivity χ_{\perp} were known, it would be straightforward to calculate the steady state τ_E and β_p .

The problem of course is that an RFP is subject to resistive MHD turbulence implying that the heat diffusivity is anomalous; that is χ_{\perp} is not known. This fundamental difficulty is overcome in the present paper by making the conjecture that the pressure rises until the profiles adjust themselves so that the plasma is marginally stable to resistive MHD modes. The marginal stability conjecture essentially provides the information necessary to determine the steady state profiles. These profiles can then be substituted into the energy balance equation to determine the anomalous χ_{\perp} that is required for self consistency.

In order to carry out the analysis just described two challenging problems have had to be overcome. The first one is associated with the marginal stability criterion against resistive MHD modes. For over three decades it has been believed that an RFP would always be unstable to resistive MHD

modes, in particular the resistive “g-mode” [3],[4]. The magnetic curvature is always unfavorable, even in a torus and thus, an unstable resistive mode would always be present even in the limit $\Delta' \rightarrow -\infty$. This well known result was derived assuming compressible MHD physics in which the energy equation reduces to the simple adiabatic relation. However, following the work of Lutjens et al on tokamaks [5] it has been shown that for an RFP the adiabatic assumption is not accurate. Instead, the thermal conductivity term dominates the contributions of compressibility and convection. The net result is that thermal conductivity tends to smooth the pressure profile, thereby providing a stabilizing mechanism against the resistive “g-mode” for sufficiently low pressure; that is there is a well defined marginal stability criterion for RFP’s against all resistive MHD modes. This includes the resistive rippling mode [6], [7] as well.

The second problem is technical in nature. The equations to be solved are highly nonlinear with strong coupling. Furthermore the marginal stability criterion depends upon $\Delta'(r)$, a local quantity whose value at any given radius depends globally upon the entire profile. Therefore, imposing marginal stability on the profiles in this case is far more difficult technically than, for instance, imposing the purely local ballooning mode criterion obtained from the well known $s - \alpha$ diagram for a tokamak. This difficulty is overcome by a numerical iteration scheme that takes advantage of the fact that the marginally stable values of plasma β are relatively small.

The net result is that the end goals of the analysis have indeed been achieved. The self consistent thermal diffusivity χ_{\perp} has been calculated for an RFP. In addition the resulting scaling relations for τ_E and β_p as functions of the plasma current I , the area integrated plasma density N , and the minor radius a have been determined and compared with various RFP data and other theories and simulations. Specifically it is shown that for an ohmically heated RFP

$$\tau_E \sim 9 \cdot 10^{-3} \cdot I^{1.1} \cdot N^{-0.25} \cdot a^{1.6} \quad (1)$$

$$\beta_p \sim 7 \cdot 10^{-2} \cdot I^{-0.75} \cdot N^{0.49} \cdot a^{-0.16} \quad (2)$$

where the units are $I[MA]$, $N[10^{20}m^{-1}]$, $a[m]$, and $\tau_E[s]$. It is also shown, perhaps surprisingly, how these results are compatible with a semiempirically derived scaling relation obtained from experimental data [8], which is of the

form

$$\tau_E \sim \left(\frac{I^2}{N}\right)^{0.25} \quad (3)$$

$$\beta_p \sim \left(\frac{N}{I^2}\right)^{0.5} \quad (4)$$

The formulation of the model and the ensuing results represent the major parts of a PhD thesis and would constitute a rather lengthy single paper. For this reason, the work is divided into two separate papers, the first one focusing on the model and the second one on the results. This paper contains a derivation of the self consistent marginally stable resistive MHD model. It contains a brief review of the previous status of resistive “g-mode” theory in addition to Taylor’s theory of relaxation. Next, the new nonlinear model is derived. Included are the main technical details concerned with solving the model. Also included is a discussion of the plasma-wall edge region, which is necessary to avoid certain spurious results in which the edge completely dominates the behavior. The final result of this paper is a set of self consistent equations describing the marginally stable RFP model along with a robust prescription for solving them numerically.

II Marginal Stability to Resistive MHD Modes in an RFP

A Pre-existing Theory

The analysis of resistive MHD modes in a cylindrical pinch has been studied extensively in the past [3],[4], and has been extended to include toroidicity effects as well [9]. In each of these works, an analytic derivation was carried out to solve the linearly perturbed resistive MHD equations in the resonant layer. A key assumption in these derivations concerned the energy equation: thermal conduction was considered negligible as compared to the convective and compressibility terms; thus the adiabatic form of the energy equation was used. Under this assumption, the following dispersion relation for resistive

MHD modes was derived:

$$r_s \Delta' = 2\pi \frac{\Gamma\left(\frac{3}{4}\right)}{\Gamma\left(\frac{1}{4}\right)} Q^{\frac{5}{4}} \left(1 - \frac{\pi D}{4Q^{\frac{3}{2}}}\right) \quad (5)$$

where r_s is the radial location of the resonance, Q is the normalized growth rate, D is Suydam's normalized pressure gradient, and Δ' is defined as the jump across the resonance of the logarithmic derivative of the radial component of the perturbed magnetic field.

It is straightforward to see that for a cylindrical pinch no stable configuration can be found in the presence of confined pressure ($D > 0$) for any value of Δ' , even $\Delta' \rightarrow -\infty$; an instability is always present (see Fig. 1a, a curve of Q vs Δ' for $D > 0$). The negative Δ' part of the curve is known as the resistive "g-mode" [4]. The same analysis performed for a toroidal geometry shows that the "g-mode" can be stabilized for magnetic configurations with sufficiently favorable average curvature (e.g. tokamaks). However, the "g-mode" remains unstable for configurations with unfavourable curvature (e.g. RFPs). The presence of the unstable "g-mode" in an RFP has been an impasse for decades in attempts to find marginal stability.

B New Theory

It is shown here that this impasse is removed by considering the effect of thermal conductivity. Based on some recent work by Lutjens et al [5] for the tokamak configuration, one can show that for a careful ordering of the resistive layer dynamics, the thermal conductivity dominates over convection and compressibility. Thus the use of the adiabatic equation of state in earlier work is not accurate for an RFP. The balancing of the thermal conductivity terms (in the parallel and perpendicular directions) dominates the perturbed energy equation and introduces a new scale length δ_χ which is proportional to the ratio of perpendicular to parallel thermal diffusivity, raised to the 1/4 power. This new scale length turns out to be much larger than the tearing mode scale length found in the earlier studies. Thermal conduction effects tend to flatten the pressure perturbation, thereby stabilizing the "g-mode".

The resulting tearing-mode dispersion relation now becomes

$$r_s \Delta' = 2\pi \frac{\Gamma\left(\frac{3}{4}\right)}{\Gamma\left(\frac{1}{4}\right)} Q^{\frac{5}{4}} - \frac{\pi^{\frac{3}{2}} D}{2 \delta_\chi} \quad (6)$$

where

$$\delta_\chi \equiv \left[\frac{\chi_\perp}{\chi_\parallel} \frac{B^2}{m^2 B_\theta^2} \left(\frac{q_s}{r_s q'_s} \right)^2 \right]^{\frac{1}{4}} \quad (7)$$

As one has come to expect, derivations of resistive MHD modes involve rather lengthy amounts of tedious algebra, which nevertheless are now more or less standard. Consequently, the details of the above derivation are not presented here but can be found in Ref [10].

A similar dispersion relation, predicting stability of the “g-mode”, was derived by Bishop et al [11] by postulating a local flattening of the equilibrium pressure profile at the resonant surface. No value was given for the width, δ_χ , which was treated as a parameter. Note that the derivation of the dispersion relation given by Eq. (6) has been obtained under the assumption of constant plasma density (which is in good agreement with experimental observations). A condition for marginal stability to resistive MHD modes is now easily found from Eq. (6) (see Fig.1b).

$$r_s \Delta' = -\frac{\pi^{\frac{3}{2}} D}{2 \delta_\chi} \quad (8)$$

Observe that the gradients in χ_\perp and χ_\parallel do not change the dispersion relation given by Eq. (6); moreover, the rippling mode [3], originating from a gradient in plasma resistivity, also can be shown to disappear in this derivation because of a change in parity of the eigenfunction.

C Taylor’s Theory of Relaxation

Once the criterion for resistive MHD marginal stability is found, it is possible to formulate a consistent model that determines the equilibrium profiles, and consequently determines the confinement properties of an ohmically heated RFP fusion experiment. The main picture that motivates the model is that

the RFP equilibrium relaxes to a driven minimum energy state, which is marginally stable against resistive MHD modes. The well known relaxation theory of Taylor [2] determines the absolute minimum energy state, in the absence of driving sources. It leads to the Bessel Function Model for the axial (B_z) and poloidal (B_θ) components of the magnetic field, together with zero pressure gradient

$$\begin{aligned} B_z &= B_0 J_0(\mu r) \\ B_\theta &= B_0 J_1(\mu r) \\ p' &= 0 \end{aligned} \tag{9}$$

Here, $\mu = \text{const}$ is related to the helicity or equivalently the reversal radius.

III Description of the Model

A The Basic Idea

Intuitively, one can visualize the idea behind the present model, leading to a finite pressure gradient extension of Taylor's minimum energy magnetic configuration. Imagine starting from one particular pure Taylor state which is positively stable against resistive MHD modes. One can then add an external heating source (ohmic heating) which raises the pressure until the plasma becomes marginally stable at every point across the radius. This idea has been supported by some experimental work, but is not conclusive. Still, it is interesting to develop a fully consistent theoretical model which determines such equilibria for an RFP configuration, and then make comparisons with the experimental results. In this section, a detailed description of the model is given, together with its computational implementation.

B The Basic Equations of the Model

1 Geometry

A cylindrical geometry with axial periodicity is adopted. Toroidicity is a second order effect in a global analysis of an RFP. Thus, the main features of an RFP equilibrium can be well described by a cylindrical model [1].

2 $B_z(r)$

A set of differential equations defining the model in cylindrical geometry is now derived and discussed. The first step is to determine the driven minimum energy state. Even though a real RFP experiment is an ohmically driven system, Taylor's non-driven relaxation theory provides a reasonably good description of the magnetic field configuration in the core of an RFP when the plasma β is low (as it turns out for our model). However, the theory does not accurately describe the profiles at the edge of the plasma since cold plasma-wall interactions are not taken into account. It is critical to treat the edge, at least quasi-realistically. The pure Taylor model which predicts a finite current density at the edge, coupled with the experimental condition of temperature vanishing at a cold wall, leads to an infinite ohmic power. Consequently the resulting energy confinement time would be zero, which is clearly not physical.

It should be recognized that including edge physics is a non-trivial task. Lacking a more general edge theory, it is assumed that the axial component of the equilibrium magnetic field $B_z(r)$ corresponds to a Taylor minimum energy state modified at the edge so that its behavior is in accordance with experimental evidence. Due to its complexity, we adopt a basic philosophy of the edge model that aims to minimize the ohmic power contribution in this region so that it is no longer a dominant effect, as it would be in the ideal Taylor model. For instance the formation of artificial pedestals or extended zero pressure gradient regions in the edge profiles are avoided. This is what might be called the "unobtrusive model for the edge".

Hereafter it is assumed that $B_z(r)$ is a known function given by Taylor over most of the plasma and modified at the edge to agree with cold-edge experimental data.

3 Pressure Balance

Thus, granted that one component of the equilibrium magnetic field is known, and characterized by several experimental operational parameters, then two profiles remain to be determined to completely describe the equilibrium configuration in a cylindrical geometry. These profiles are $B_\theta(r)$ (which is nearly a Taylor profile) and $p(r)$. MHD force balance provides one obvious relation-

ship between these quantities:

$$B_z B'_z + \frac{B_\theta}{r} (r B_\theta)' + \mu_0 p' = 0 \quad (10)$$

4 Marginal Stability

The second relation is given by the marginal stability condition, Eq. (8). Strictly speaking, this condition holds only at the resonant surfaces on which Δ' is evaluated. In a periodic cylindrical geometry, the resonant surfaces are discrete for a given aspect ratio R/a ; that is for a particular device. However, the resistive MHD eigenfunctions are global in nature, practically extending over the entire plasma region. This eigenfunction overlap suggests that using Eq. (8) as a continuum rather than discrete constraint may be a reasonable approximation. In short, in the model the marginality condition is imposed continuously at every radial location in the plasma region.

Thus, Eq. (8) is a differential equation relating several plasma quantities; in particular, it is a relationship involving not only $B_\theta(r)$ and $p(r)$, but also the thermal diffusivities in the parallel and perpendicular direction. Because of the enormity of its size, it is plausible to assume that $\chi_{||}$ is given by its classical value. It is so large that there is no need for anomalies. However, χ_{\perp} is anomalous. Thus, marginal stability represents an additional constraint equation on the equilibrium, but also introduces another unknown χ_{\perp} .

Finally, Eq. (8) shows a dependence on the poloidal mode number m as well. This dependence suggests that a marginally stable pressure profile can be built for each mode m . It is easy to see, though, that $m = 1$ is the most stringent poloidal mode, thus providing the smallest marginally stable pressure gradient.

5 Energy Balance

Further physics needs to be added in order to close the system. This physics arises from the requirement that perpendicular transport must be consistent with the resulting pressure gradient as determined from energy balance

$$\frac{1}{r} (r n \chi_{\perp} T')' = -\eta j^2 \quad (11)$$

In Eq. (11) the plasma resistivity is assumed to be classical in accordance with experimental data. The system has now been closed in a self consistent

manner using the classical values of $\chi_{||}$ and η given by

$$\chi_{||} = \frac{\hat{\chi}_{||} T_k^{\frac{5}{2}}}{n_{20}} \quad [m^2/s] \quad (12)$$

$$\eta = \hat{\eta} T_k^{-\frac{3}{2}} \quad [\Omega - m] \quad (13)$$

where

$$\hat{\chi}_{||} = 5.44 \cdot 10^8 \quad (14)$$

$$\hat{\eta} = 3.32 \cdot 10^{-8} \quad (15)$$

The plasma temperature T_k is expressed in $[keV]$, the density n_{20} in $[10^{20} m^{-3}]$, and all other quantities are given in MKS units. It should be emphasized that the perpendicular heat transport is not going to be classical, as the self-consistently determined χ_{\perp} will turn out to be much higher (about two orders of magnitude in the plasma core) than its classical value as found in Ref. [12]. In spite of its simplicity, one of the attractive features of this model lies in its ability to quantitatively determine the radial profile for $\chi_{\perp}(r)$ consistent with the marginally stable equilibrium.

6 Summary of Equations

Finally, the closed set of differential equations, whose unknowns are $B_{\theta}(r)$, $T(r)$, and $\chi_{\perp}(r)$ can be rewritten as

$$B_z B'_z + \frac{B_{\theta}}{r} (r B_{\theta})' + \mu_0 p' = 0 \quad (16)$$

$$\frac{1}{r} (r n \chi_{\perp} T')' = -\eta j^2 \quad (17)$$

$$\frac{\mu_0 p'}{\chi_{\perp}^{\frac{1}{4}}} = \frac{\Delta' B_z^2}{\pi^{\frac{3}{2}} \chi_{||}^{\frac{1}{4}}} \sqrt{\frac{B}{m B_{\theta}}} \left(\left| 1 + \frac{r B'_z}{B_z} - \frac{r B'_{\theta}}{B_{\theta}} \right| \right)^{\frac{3}{2}} \quad (18)$$

where $p = nT$ is the plasma pressure and B_z is assumed to be known. The plasma density n is assumed to be a known constant, in good agreement with experimental observations. Finally the current density satisfies Ampere's law $\nabla \times \mathbf{B} = \mu_0 \mathbf{j}$, while m is the poloidal mode number (set to $m = 1$, the most unstable mode).

Note that the system of Eqs. (16)-(18) is highly nonlinear. However, the main difficulty arises from the appearance of $\Delta'(r)$, a local quantity which nevertheless requires global information for its calculation. This makes the numerical solution of Eq. (16) quite challenging. In the present work, an iterative approach has been used to solve Eq. (16): the basic assumption is that the plasma pressure will turn out to be small ($\beta_p \ll 1$), as suggested by the experiments. This assumption dramatically simplifies the solution procedure, as is shown next. Moreover, the convergence of the method turns out to be quite fast. The resulting equilibrium pressure is shown, a posteriori, to be small as assumed.

C The Solution Procedure

1 General Considerations

If the plasma has zero pressure gradient, then $B_\theta(r)$ can be evaluated immediately by numerically integrating the MHD force balance, since B_z is an assigned Taylor-like function in the model. Furthermore, Δ' can also be easily evaluated numerically with zero pressure gradient, yielding the dependency for Δ' on the (continuous) radial location of the resonant surface:

$$\Delta' = \Delta'_0(r) \quad (19)$$

Once $\Delta'_0(r)$ is known, the other two unknowns $T_k(r)$ and $\chi_\perp(r)$ can be found by numerically solving the remaining Eqs. (16)-(18), which now can be written as

$$T_k^{\frac{3}{2}} \frac{d}{dr} \left(r n_{20} \chi_\perp \frac{dT_k}{dr} \right) = -\eta_0 j_\parallel^2 r \quad (20)$$

$$\frac{T_k^{\frac{5}{8}}}{\chi_\perp^{1/4}} \frac{dT_k}{dr} = g(r) \equiv \frac{B_z^2 \Delta'_0}{n_{20}^{\frac{3}{4}} \chi_0^{\frac{1}{4}}} \sqrt{\frac{B}{m B_\theta}} \left| 1 + \frac{r B'_z}{B_z} - \frac{r B'_\theta}{B_\theta} \right|^{\frac{3}{2}} \quad (21)$$

where $\eta_0 = \frac{\hat{\eta}}{e \cdot 10^{23}} = 2.08 \cdot 10^{-12}$, and $\chi_0 = \hat{\chi}_\parallel \left[\mu_0 10^{23} \pi^{\frac{3}{2}} \right]^4 = 8.54 \cdot 10^4$.

Notice that in order to solve Eq. (20) and Eq. (21), the value of temperature on axis T_0 must be given; since this value is ultimately determined by the boundary condition at the wall $T|_a = 0$, the solution procedure then involves an initial guess for T_0 . The algorithm described here is then iteratively

repeated by adjusting the initial guess of T_0 until the condition $T|_a = 0$ is satisfied.

The procedure for constructing the pressure profile is now described in detail. In carrying out this procedure it is helpful to keep in mind a typical Δ'_0 profile, as shown in Fig. 2, together with the analytic expressions for Δ'_0 valid on axis and at the reversal layer

$$\Delta'_0|_{r \simeq 0} \sim -\frac{1}{r} \quad ; \quad \Delta'_0|_{r \simeq r_0} \sim -\frac{1}{|r - r_0|} \quad (22)$$

This is important because Eq. (21), which is valid over most of the profiles, does not represent the most stringent pressure limitation over the entire profile. In particular, near the axis and the reversal layer stricter constraints apply and the self consistent pressure profile is always determined using the most severe criterion.

2 Criterion near the axis

By expansion around $r = 0$, it is easy to show that the analytic solution of Eqs. (20) and (21) near $r \sim 0$ yields the following behavior for the pressure profile

$$p'|_{r \simeq 0} \sim r^{\frac{7}{5}} \quad (23)$$

This pressure gradient, however, turns out to be unstable to ideal MHD modes; in particular, it violates Suydam's criterion on axis [13]:

$$\mu_0 p' = -\frac{B_z^2}{8r} \left[1 + \frac{r B'_z}{B_z} - \frac{r B'_\theta}{B_\theta} \right]^2 \Rightarrow p'|_{r \simeq 0} \sim r^3 \quad (24)$$

As Eq. (24) shows, Suydam's criterion for marginal stability to ideal MHD modes forces the pressure to be very flat on axis, much flatter than Eq. (21) would require. This suggests that the equilibrium profiles for pressure (or equivalently temperature) and χ_\perp on axis will be determined by Suydam's criterion, and not by Eq. (23).

As the solution for the profiles evolves away from the axis, Δ'_0 becomes finite and smaller. This reduces the pressure gradient generated by the resistive MHD marginality condition, until eventually it becomes smaller than the gradient generated by Suydam's condition. At the radial location where

the resistive MHD marginality condition becomes more restrictive than Suydam's, a transition occurs, such that the pressure and corresponding χ_{\perp} are always determined by the most restrictive criterion everywhere in the plasma region. Thus, near $r \sim 0$ the resistive MHD marginal stability criterion Eq. (21) is replaced by Suydam's criterion.

From a numerical point of view, it is easier to locate this transition by looking at the thermal diffusivity rather than the pressure gradient. Having established that p' on axis is given by Suydam's criterion, p' can be immediately evaluated via Eq. (24); χ_{\perp} is then found directly from integrating the power balance given by Eq. (20). The transition can easily be found by comparing this χ_{\perp} with the corresponding function $\chi_{\perp,T-M}$ that would result from the resistive MHD marginal condition Eq. (21) for the same profile of Suydam-marginal pressure gradient:

$$\chi_{\perp,T-M} = \left[\frac{T' T^{\frac{5}{8}}}{g(r)} \right]^4 \quad (25)$$

One can easily show that on axis $\chi_{\perp} \sim r^{-2}$, while $\chi_{\perp,T-M} \sim r^6$, so that it is straightforward to distinguish among the two quantities. The radial location where the two functions eventually intersect, defines the transition point r_1 (see Fig. 3); for $r > r_1$, T' and χ_{\perp} will be determined by the tearing-mode marginality condition (which will now be the most restrictive criterion).

3 Criterion near Reversal Point

A similar expansion around the axial field reversal point r_0 can also be carried out. This also leads to an analytic solution for Eqs. (20) and (21). In this case, $B_z = B'_z|_{r_0} (r - r_0) + O(r - r_0)^2$, while $B_{\theta} = B_{\theta}|_{r_0}$ and $\mu_0 j_{\parallel} = -(B_{\theta} B'_z)|_{r_0}$ are finite quantities. Moreover, as shown in Eq. (22), $\Delta'_0 \sim -|r - r_0|^{-1}$. Thus $g \sim |r - r_0|^{-1/2}$. By taking $T = T_0 + T_1 |r - r_0|^{\alpha}$, Eqs. (20) and (21) then give

$$\begin{aligned} \chi_{\perp} T' &\sim |r - r_0|^0 \\ \chi_{\perp} &\sim T'^4 |r - r_0|^2 \end{aligned} \quad \Rightarrow \quad \begin{aligned} \chi_{\perp} &\sim |r - r_0|^{2/5} \\ T' &\sim |r - r_0|^{-2/5} \end{aligned} \quad (26)$$

As the reversal point is approached, the temperature gradient given by Eq. (21) becomes steeper and steeper, eventually approaching infinity; this implies that there will be a thin region around $r = r_0$ where the tearing-mode

marginal pressure gradient profile again exceeds Suydam's limit. Similar to the behavior on axis, the model passes through a transition region in which the pressure gradient around r_0 is determined by Suydam's marginal condition (24). As is shown later, from a numerical point of view this region is very localized around $r = r_0$ due to the weak dependency of p' on $r - r_0$, and also due to the relatively large value of Suydam's pressure gradient limit with respect to the typical tearing-mode marginal pressure gradient in the plasma core. Thus in practical simulations, involving on the order of five hundred radial grid points, this transition to Suydam's criterion can be ignored. It is blurred by small but finite numerical resolution.

4 Considerations concerning the solution near the Edge

As the evaluation of the profiles evolves past the reversal point, p' again becomes finite and is determined by tearing-mode marginality until the edge region is approached. As shown in Fig. 2, $\Delta'_0|_{r \rightarrow a} \rightarrow -\infty$, due to the presence of the ideal wall which provides a strong artificial stabilizing effect at the plasma boundary ($r \sim a$). A resistive wall would not exhibit this stabilization. However, an accurate treatment of the edge is quite complicated. For present purposes, it is necessary to determine the radial location $r = r_2$ at which the resistive MHD marginality model loses validity due to the artificially stabilizing effect of the ideal wall. This location sets the final transition point, between the resistive MHD marginally stable region and the plasma edge region which is then defined by $r_2 < r < a$.

As mentioned earlier, in the plasma edge region additional physics needs to be introduced. For the sake of simplicity, in the present model an analytical smoothing of the profiles is used for $r_2 < r < a$, by imposing appropriate matching conditions at $r = r_2$ and appropriate boundary conditions at $r = a$. In the next section it is shown in detail that this continuation of the profiles is suggested by experimental observations, in conjunction with the idea of the "unobtrusive edge". The model avoids the formation of artificial pedestals or flattened regions in the edge profiles. In essence the details of the smoothing become unimportant because the edge region is narrow and the artificial singularity in the ohmic power P_Ω due to the conditions of finite $j_{||}$ and $T = 0$ is removed. But before discussing these details, however, the iterative process is now described.

5 Iteration Process

After having found $B_\theta(r)$, $p(r)$, and $\chi_\perp(r)$ for $0 < r < a$ in the first iteration, it is straightforward to repeat the procedure for the second iteration by simply substituting the pressure profile just obtained into the RHS of Eq. (21). This involves recalculating Δ' with a non-zero pressure (see Fig. 2). Then, the second iteration is performed by following exactly the same steps as the first one, leading to new profiles for $p(r)$ and χ_\perp . Convergence, basically measured by the change in the global parameters of plasma confinement, is quickly reached at the end of the second iteration.

D The Edge

1 The Edge Problem

As stated previously, considerable care must be devoted to the edge region to eliminate the artificial singularity that arises in $P_\Omega \sim j_\parallel^2/T^{3/2}$ when j_\parallel is finite and $T \rightarrow 0$ because of the cold edge boundary condition. Furthermore the edge profiles should not introduce artificial pedestals or overly flattened profiles. Lastly, it is desirable to have a model in which small, but finite values of T , j , and n are not required, in order to keep the results uncluttered with small parameters difficult to determine. In essence a considerable effort is required to make the edge unobtrusive. The profiles should be physically plausible, independent of small parameters, and not affect the global values of τ_E and β_p . The edge model described here meets these requirements. There are two main issues: (1) where does the edge begin and (2) what are the appropriate jump conditions and edge radial functions that satisfy the edge boundary conditions? These two issues are addressed below.

2 The $B_z(r)$ field

Consider first the specification of $B_z(r)$ which is given as an input. It must be properly chosen so that it describes a minimum energy state as given by Taylor's theory, and at the same time takes into account the presence of the wall at $r = a$. Experiments indicate that at the wall the plasma current density, pressure and pressure gradient drop dramatically from their respective values in the plasma core region. The presence of a wall thus mainly cools the plasma at the edge; this feature is not contained in Taylor's theory, for the BFM predicts finite current densities at $r = a$. Although j , p , p' , and T

do not completely vanish at the wall, it is convenient to ignore these small values and impose the following universal boundary conditions at the wall:

$$\mathbf{j}|_a = 0 \quad ; \quad p'|_a = 0 \quad ; \quad p|_a = 0 \quad ; \quad T|_a = 0 \quad ; \quad (27)$$

An appropriate choice for $B_z(r)$ that takes into account Eq. (27) is given in terms of $j_\theta \sim B'_z$. Specifically it is assumed that

$$B'_z(r) = -B_{z0}\mu J_1(\mu r) \cdot \left[\frac{\tanh \left[f \left(1 - \frac{r^2}{a^2} \right) \right]}{\tanh(f)} \right]^\nu \quad (28)$$

where $\mu = \text{const}$ is related to the helicity (or the field reversal point, or the plasma current). This function is the product of the BFM solution (see Eq. (9)) and an edge term, described by the hyperbolic tangent (see Fig. 4), such that the resulting profile will coincide with Taylor's relaxed state in the plasma core, while being modified only at the edge in order to automatically satisfy the condition of vanishing current density at the wall (see Eq. (27)). Two free parameters, f and ν , appear in the edge term: basically, f defines the radial location of the boundary between core and edge region, while ν determines how rapidly the profiles approach zero right at the wall. Using physical requirements, one can now provide a prescription that uniquely determines f and ν .

3 The radial location of the edge

The first step is to determine the radial location $r = r_2$ at which the edge region begins. As previously mentioned, in the model the plasma edge is the region in which the stabilizing effect due to the perfectly conducting wall becomes significant in the determination of the plasma profiles. This stabilising effect is 'artificial': it appears as a large and negative (i.e. very stable) Δ' (see Fig. 2) at $r \cong a$, which would generate a large pressure gradient (and corresponding pedestal) near the wall, were the resistive MHD marginality condition applied.

Based on this insight, a reasonable way to determine r_2 is obtained by examining the typical Δ' profile (see Fig. 5). Here r_2 is defined as the radial location between the reversal point $r = r_0$ and the wall $r = a$, at which Δ'_0 (that is the Δ' calculated in the first iteration, with zero pressure) has a maximum. In this way, the resistive MHD marginality condition is not used

to determine the plasma profiles in the region near the wall where Δ' becomes large and negative. This procedure avoids the 'artificially' stabilizing wall effect. Once r_2 is defined, a natural prescription for determining the free parameter f can be devised: f is chosen such that the edge term introduced in Eq. (28), evaluated at $r = r_2$, is equal to half its value on axis

$$\frac{\tanh \left[f \left(1 - \frac{r_2^2}{a^2} \right) \right]}{\tanh(f)} = \frac{1}{2} \quad (29)$$

Since Δ'_0 depends on f (through B_z), some iteration is initially required at the beginning of each simulation in order to find f . This iteration is straightforward. Also the global parameters τ_E and β_p are insensitive to the choice "1/2".

4 Determining ν

What remains now is to give a prescription for ν to completely define the model. The free parameter ν basically determines the rate at which the plasma profiles approach zero right at the wall $r \cong a$. In particular note that

$$B'_z(r \cong a) \sim \left(1 - \frac{r}{a} \right)^\nu \quad (30)$$

Aside from the boundary conditions (27), an additional constraint at the wall arises from Ohm's Law:

$$\mathbf{E} + \mathbf{v} \times \mathbf{B} = \eta \mathbf{j} \quad (31)$$

The electric field at $r = a$ must be finite, implying that

$$T^{\frac{3}{2}} \sim j \sim \left(1 - \frac{r}{a} \right)^\nu \quad (32)$$

based on Spitzer's formula for plasma resistivity. Furthermore, MHD force balance requires that near $r \sim a$

$$p' \sim B'_z \sim \left(1 - \frac{r}{a} \right)^\nu \Rightarrow p \sim \left(1 - \frac{r}{a} \right)^{\nu+1} \quad (33)$$

Thus in the edge region the plasma density can no longer be constant, but has to vanish at the wall

$$n \sim \left(1 - \frac{r}{a} \right)^{\frac{\nu}{3}+1} \quad (34)$$

The edge region is thus highly constrained and in fact only a small range in ν is physically acceptable: $1 < \nu < 3/2$. For $\nu < 1$ there are pedestals in j and T while for $\nu > 3/2$ there is an artificial flattening of T and p' . The prescription used in the model leaves j_{\parallel} unchanged during iterations from the force free case using the edge modified B_z and determining B_{θ} from pressure balance. The pressure gradient is continuous at $r = r_2$ through p'' while the temperature is continuous through T' . The resulting profiles are quite smooth through $r = r_2$ and approach zero at $r = a$ without pedestals or overly flattened regions. The global parameters are insensitive to the choice of ν as long as ν lies between 1 and $3/2$. The specific edge profiles valid for $r > r_2$ are given by

$$p' = A_1 \left(\frac{a-r}{a-r_2} \right)^{\nu} - A_2 \left(\frac{a-r}{a-r_2} \right)^{\nu+1} \quad (35)$$

$$T = A_3 \left(\frac{a-r}{a-r_2} \right)^{\frac{2}{3}\nu} - A_4 \left(\frac{a-r}{a-r_2} \right)^{\frac{2}{3}\nu+1} \quad (36)$$

$$j_{\parallel} = \frac{j_{\theta} B_{\theta} + j_z B_z}{B} \quad (37)$$

where

$$\begin{aligned} A_1 &\equiv p'|_{r_2}(1+\nu) + p''|_{r_2}(a-r_2) \\ A_2 &\equiv \nu p'|_{r_2} + p''|_{r_2}(a-r_2) \\ A_3 &\equiv \left(\frac{2}{3}\nu + 1 \right) T|_{r_2} + T'|_{r_2}(a-r_2) \\ A_4 &\equiv \frac{2}{3}\nu T|_{r_2} + T'|_{r_2}(a-r_2) \end{aligned} \quad (38)$$

In the numerical results the value $\nu = 1$ is used.

IV Summary

The details of the model and the method of solution have been described. Although the resistive MHD marginal stability is valid over the great majority of the profile, there are narrow layers near the axis, the reversal point, and the wall that require special treatment. This leads to a somewhat complicated model and it is appropriate to end the first paper with a complete summary

of the model in one place. The summary includes the setting up of the problem, the solution in the special layer regions, and the resistive MHD marginal model.

A Setting up the problem

To start the problem one specifies the values of density n_0 and wall radius a . The minimum energy-edge modified $B'_z(r)$ is given by

$$B'_z(r) = -B_{z0}\mu\hat{J}_1(\mu r) \cdot \left[\frac{\tanh \left[f \left(1 - \frac{r^2}{a^2} \right) \right]}{\tanh(f)} \right]^\nu \quad (39)$$

Here B_{z0} and μ are specified constants which are related to the plasma current I and the location of the reversal layer $r = r_0$ at the completion of the calculation. In accordance with the edge model the value of ν is chosen as $\nu = 1$. The parameter f is guessed initially and then determined by iteration as described shortly. Eq. (39) is integrated subject to $B_z(0) = B_{z0}$ to determine $B_z(r)$. The poloidal field $B_\theta(r)$ is determined next from pressure balance

$$B_\theta^2 = -\frac{1}{r^2} \int_0^r r^2 \frac{dB_z^2}{dr} dr \quad (40)$$

The pressure contribution from a previous iteration can easily be added to Eq. (40). Knowing $B_z(r)$ and $B_\theta(r)$ (and $p(r)$ from the previous iteration) allows one to calculate $\Delta'_0(r)$. The value of the parameter f is determined by iterating this procedure until

$$\frac{\tanh \left[f \left(1 - \frac{r_2^2}{a^2} \right) \right]}{\tanh(f)} = \frac{1}{2} \quad (41)$$

where r_2 is the location of the core-edge transition corresponding to the maximum in Δ'_0 in the region between the reversal and the wall. The net result is that one now knows $B_z(r)$, $B_\theta(r)$, and Δ'_0 at the end of this procedure (for any given iteration).

B The region near the axis

The region near the axis is dominated by Suydam's criterion. In this region the pressure (or temperature) and thermal diffusivity are determined by solving

$$2.0 \cdot 10^{-2} \cdot n_{20} T'_k = -\frac{B_z^2}{8r} \left[1 + \frac{r B'_z}{B_z} - \frac{r B'_\theta}{B_\theta} \right]^2 \quad (42)$$

$$\chi_\perp = \chi_{\perp,S} = -\eta_0 \frac{1}{r n_{20} T'_k} \int_0^r \frac{j_{\parallel}^2}{T_k^{3/2}} r \, dr \quad (43)$$

The value of temperature on axis $T(0) = T_0$ is guessed and then iterated to satisfy the edge condition $T(a) = 0$. As these equations are integrated away from the axis, the value of χ_\perp implied by resistive MHD marginal stability is also evaluated as follows

$$\chi_{\perp,T-M} = \left[\frac{T'_k T_k^{5/8}}{g(r)} \right]^4 \quad (44)$$

where $g(r)$ is given by Eq. (21) with $m = 1$ corresponding to the worst mode. In this region $\chi_{\perp,T-M} < \chi_{\perp,S}$.

C The core region

The Suydam solution is valid over a narrow region near the axis, $0 < r < r_1$. The radius r_1 corresponds to the point where $\chi_{\perp,T-M}$ just exceeds $\chi_{\perp,S}$. Once this occurs, the resistive MHD marginal stability model is dominant and χ_\perp and T_k are determined by simultaneously solving

$$\frac{1}{r} \frac{d}{dr} \left(r \chi_\perp \frac{dT_k}{dr} \right) = -\frac{\eta_0}{n_{20}} \frac{j_{\parallel}^2}{T_k^{3/2}} \quad (45)$$

$$\frac{dT_k}{dr} = g(r) \frac{\chi_\perp^{1/4}}{T_k^{5/8}} \quad (46)$$

The starting conditions require that T_k , T'_k and χ_\perp are continuous across $r = r_1$. The solution to these equations remains valid up until the core-edge transition $r = r_2$. Strictly speaking a modified layer near the reversal

surface should be included, but the layer is so narrow that numerical dissipation smooths out the solution with negligible impact on the macroscopic parameters.

D The edge region

In the edge the pressure gradient and temperature are modeled as follows

$$p' = A_1 \left(\frac{a-r}{a-r_2} \right)^\nu - A_2 \left(\frac{a-r}{a-r_2} \right)^{\nu+1} \quad (47)$$

$$T = A_3 \left(\frac{a-r}{a-r_2} \right)^{\frac{2}{3}\nu} - A_4 \left(\frac{a-r}{a-r_2} \right)^{\frac{2}{3}\nu+1} \quad (48)$$

The coefficients A_j are given by Eq. (38) and guarantee that p' , p'' , T , and T' are continuous across $r = r_2$. The pressure is found by integrating Eq. (47) assuming as a starting condition continuity in p across r_2 . In general the resulting pressure will not satisfy $p(a) = 0$. The starting guess for $T(0) = T_0$ is then refined, and the procedure iterated until $p(a) = 0$. This then completes the solution for a given set of input parameters. The results obtained by this procedure are discussed in the next paper.

References

- [1] H. A. B. Bodin and A. A. Newton. *Nucl. Fusion*, **20**:1255, 1980.
- [2] J. B. Taylor. *Phys. Rev. Lett.*, **39**:139, 1974.
- [3] H. B. Furth, J. Killeen, and M. N. Rosenbluth. *Phys. Fluids*, **6**:459, 1963.
- [4] B. Coppi, J. M. Greene, and J. L. Johnson. *Nucl. Fusion*, **6**:101, 1966.
- [5] H. Lutjens, J.F. Luciani, and X. Garbet. *Phys. Plasmas*, **8**:4267, 2001.
- [6] L. Garcia, P. H. Diamond, B. A. Carreras, and J.D. Callen. *Phys. Fluids*, **25**:2147, 1985.
- [7] B. A. Carreras, P. W. Gaffney, H. R. Hicks, and J.D. Callen. *Phys. Fluids*, **28**:1231, 1982.
- [8] M. R. Stoneking, S. T. Chapman, et al. *Phys. of Plasmas*, **5**:1004, 1998.
- [9] J. L. Johnson A. H. Glasser, J. M. Greene. *Phys. Fluids*, **18**:875, 1975.
- [10] A. Bruno. Tearing-mode transport model in the reversed field pinch concept. *PhD Thesis - MIT PSFC*.
- [11] C. M. Bishop, J. W. Connor, R. J. Hastie, and S. C. Cowley. *Plasma Phys. Controlled Fusion*, **33**:389, 1991.
- [12] S. I. Braginskii. In *Reviews of Plasma Physics*, volume 1. Consultants Bureau, NY, 1965.
- [13] J. P. Freidberg. *Ideal Magnetohydrodynamics*. Plenum Press-NY, 1987.

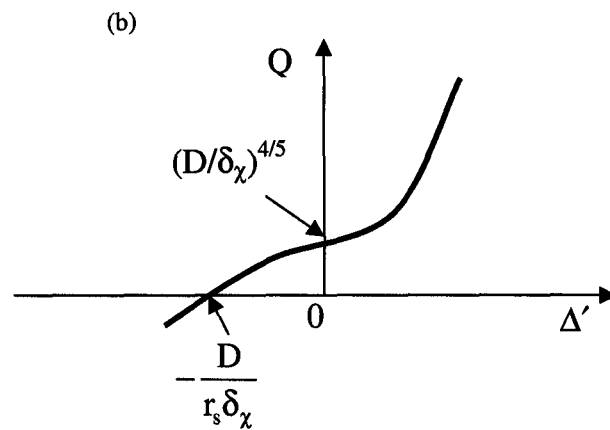
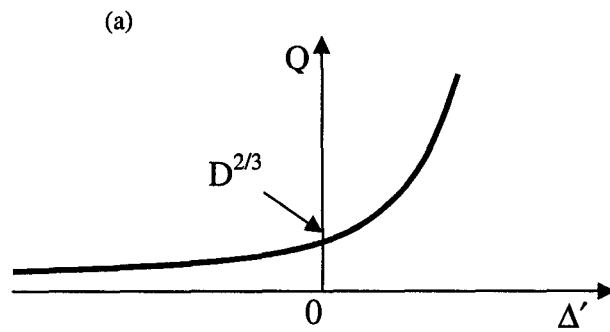


Figure 1: Schematic of the curve Q vs. Δ' for $D > 0$ as described by (a) Eq. (5) and (b) Eq. (6)

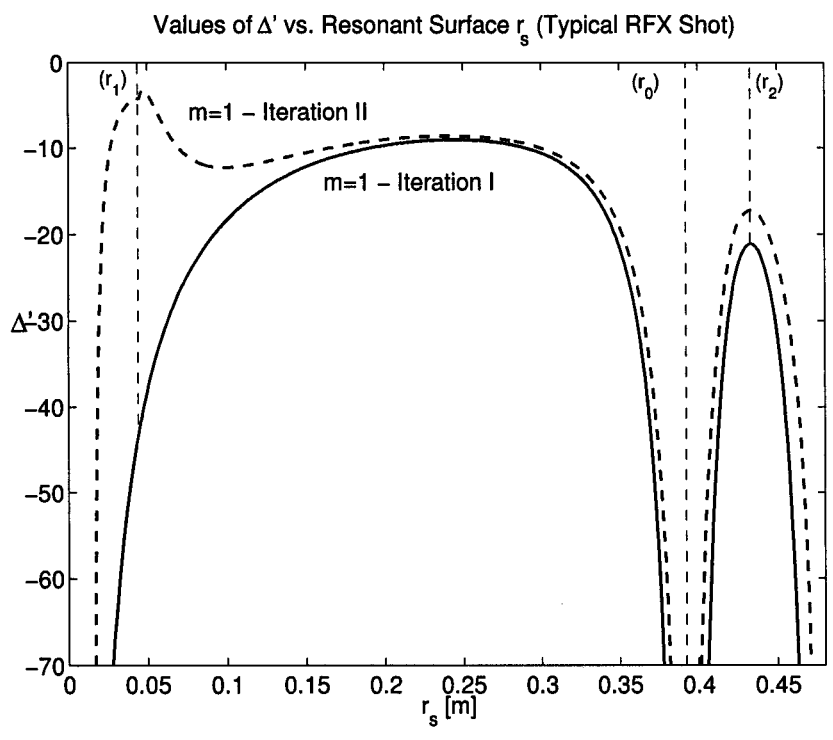


Figure 2: Illustration of the Transport Model Iterative Solution Procedure

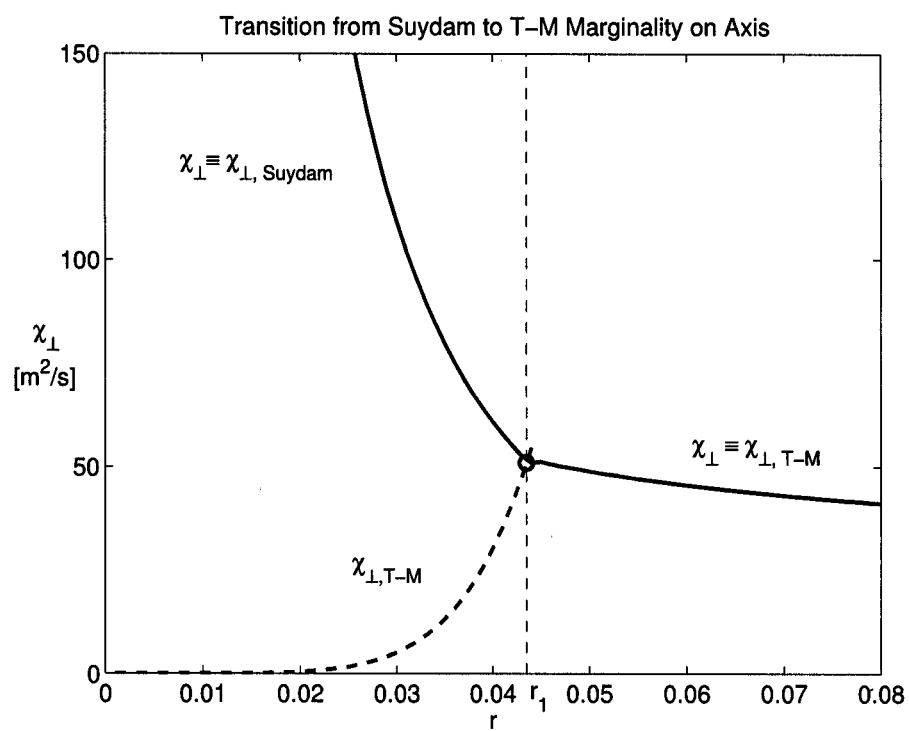


Figure 3: Determination of the Transition Point r_1

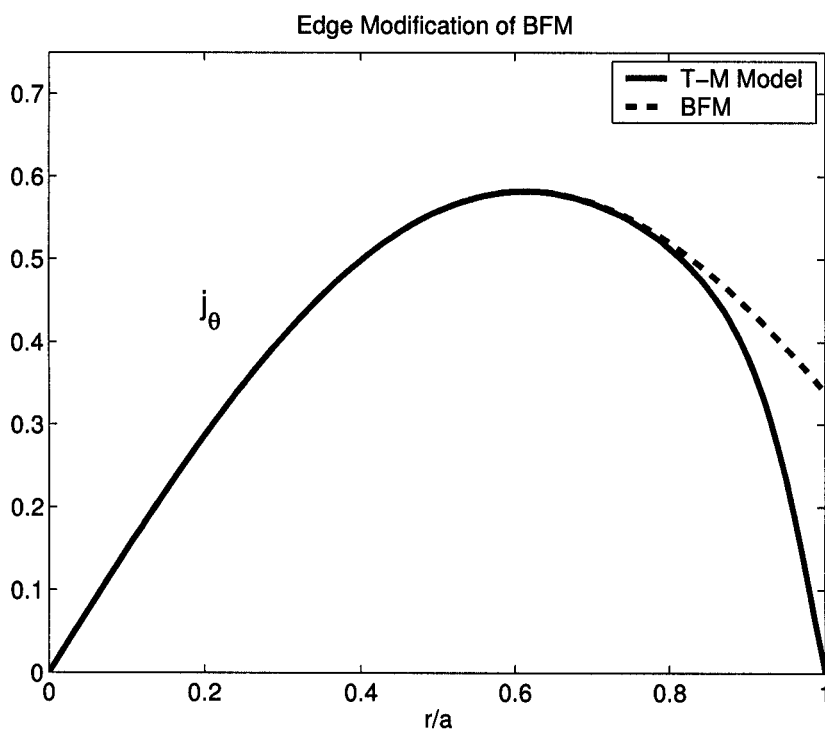


Figure 4: Edge Modified Profile for j_θ as in Equation (28)

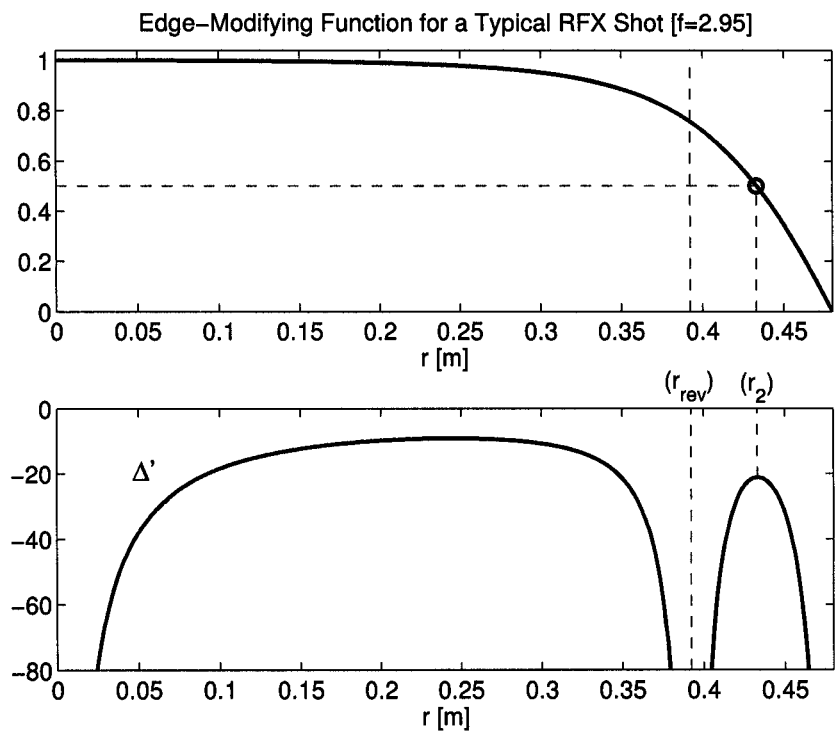


Figure 5: Determination of f and the Edge Region $r > r_2$